



HAL
open science

Niobium- and bismuth-silver phosphate glasses for the conditioning of radioactive iodine

Anne Lise Chabauty, Lionel Campayo, François Mear, Lionel Montagne

► **To cite this version:**

Anne Lise Chabauty, Lionel Campayo, François Mear, Lionel Montagne. Niobium- and bismuth-silver phosphate glasses for the conditioning of radioactive iodine. *Journal of Non-Crystalline Solids*, 2019, 510, pp.51-61. 10.1016/j.jnoncrysol.2019.01.015 . hal-02462147

HAL Id: hal-02462147

<https://hal.univ-lille.fr/hal-02462147v1>

Submitted on 31 Jan 2020

HAL is a multi-disciplinary open access archive for the deposit and dissemination of scientific research documents, whether they are published or not. The documents may come from teaching and research institutions in France or abroad, or from public or private research centers.

L'archive ouverte pluridisciplinaire **HAL**, est destinée au dépôt et à la diffusion de documents scientifiques de niveau recherche, publiés ou non, émanant des établissements d'enseignement et de recherche français ou étrangers, des laboratoires publics ou privés.

Niobium- and Bismuth-Silver Phosphate Glasses for the Conditioning of Radioactive Iodine

A.-L. Chabauty^{1,2}, L. Campayo², F. O. Méar¹, L. Montagne¹

(1) Univ. Lille, CNRS, Centrale Lille, ENSCL, Univ. Artois, UMR 8181 - UCCS - Unité de Catalyse et Chimie du Solide, F-59000 Lille, France.

(2) CEA, DEN, DE2D/SEVT/LDMC – Marcoule, F-30207 Bagnols-sur-Cèze, France.

Abstract

Iodine 129 is a radioactive waste coming from the nuclear industry. Due to its high volatility, it cannot be vitrified in conventional borosilicate glasses. As a part of the assessment of alternative solutions, this work focuses on the study of the feasibility of iodine conditioning using a glass matrix aiming at a long-term storage in a geological repository. Silver phosphate glasses, which can incorporate high amounts of iodine and can be synthesized at low temperature, were chosen for this study. In order to increase their chemical durability, these glasses were crosslinked by niobium and bismuth oxides. Niobium and bismuth incorporation limits were determined for an iodine amount of 12 wt% and range from 1.6 mol% to 4.0 mol%, depending on the $\text{Ag}_2\text{O}/\text{P}_2\text{O}_5$ ratio. The glasses polymerization state was investigated using ^{31}P MAS NMR, RAMAN spectroscopy and X-ray absorption spectroscopy. Iodine local environment was determined by EXAFS at iodine K-edge. Structural investigations show that the introduction of those crosslinking reagents induces a significant increase of the polymerization degree of the glasses. However, despite this higher connectivity, the two crosslinking reagents have a low impact on the glass transition temperature of iodine-containing silver phosphate glasses.

1. Introduction

Nuclear power plants are an effective way of producing energy with low greenhouse gas emission. However, they generate radioactive waste that must be managed to minimize its impact on the environment and human health. High level nuclear waste is usually vitrified in borosilicate glasses so that it can eventually be stored in a deep geological repository.

Radioactive iodine ^{129}I , which results from the fission of uranium 235 atoms, has a very long half-life of 15.7×10^6 years and is highly mobile in geological environments generally considered for storage purposes [1]. Thus, it is of critical importance to ensure its safe conditioning in a highly durable matrix. During the spent nuclear fuel treatment, iodine can be trapped on silver nitrate -impregnated filters and then be recovered as silver iodide. However, silver iodide is volatile above $650\text{ }^\circ\text{C}$ and cannot be vitrified with high level nuclear waste, as nuclear borosilicate glasses require to be synthesized at least at $1100\text{ }^\circ\text{C}$ [2].

Several matrices have been suggested for a specific conditioning of radioactive iodine, the most studied being lead-vanadium apatite [3], iodate-substituted hydroxyapatite [4], sodalites [5], cements [6], phosphate glasses [7] as well as composite materials [8]. Phosphate glasses are known for their low melting temperature as well as their ability to accommodate high loadings of iodine (up to 65 mol% AgI) [9]. These particularly low melting temperatures can be explained by the low polymerization degree of the glass network induced by the pentavalency of phosphorus, unlike borosilicate glasses which can reach higher polymerization degrees. However, this also means that phosphate glasses are known for being less resistant to hydrolysis, and therefore to alteration in an aqueous medium. As such, phosphate glasses could not be considered as suitable for long term storage in a geological repository.

However, a number of methods can be considered to enhance the chemical durability of these glasses, relying on the modification of the glass network polymerization degree, such as nitridation [10], which consists in the substitution of oxygen by nitrogen, or the addition of crosslinking reagents, which are multivalent oxides able to form new bonds between the phosphate chains and thus to increase the polymerization degree of the glass network. Several oxides show good results in enhancing the chemical durability of phosphate glasses, including Fe_2O_3 [11], Al_2O_3 [12], Bi_2O_3 [13] and Nb_2O_5 [14]. Fe_2O_3 -containing phosphate glasses in particular have shown sufficient durability properties for the conditioning of radioactive waste [15].

Considering that iodine is provided in the form of silver iodide, it was decided to focus on silver phosphate glasses for a specific conditioning of iodine. Previous studies on silver aluminophosphate glasses [16] showed that while Al_2O_3 was soluble in silver phosphate glasses, the addition of iodine leads to the formation of crystallized $\text{Al}(\text{PO}_3)_3$ phases, thus limiting the amount of Al_2O_3 that can be added to these glasses. Consequently, the chemical durability enhancement brought by the addition of Al_2O_3 is low [17]. Bi_2O_3 has displayed a higher incorporation limit in the same glasses [18]. It was hypothesized that this better incorporation was linked to the higher polarizability of Bi^{3+} ions (6.12 \AA^3 against 0.79 \AA^3 for Al^{3+} [19]), allowing them to better accommodate the network distortion induced by the addition of AgI into the glass.

Following this, we decided to optimize the glass composition of Bi_2O_3 -containing silver phosphate glasses. We also decided to study the incorporation limit of Nb_2O_5 in silver phosphate glasses, as Nb^{5+} also have a higher polarizability than Al^{3+} (3.97 \AA^3 [19]). In doing so, we focused on two set of compositions: AgPO_3 ($\text{Ag/P} = 1$) and $\text{Ag}_5\text{P}_3\text{O}_{10}$ ($\text{Ag/P} = 1.6$), to

which we added the crosslinking reagents in order to compare their incorporation limit for each Ag/P ratio. A detailed study of their thermal properties and their structure was carried out to determine the effect of these oxides on the glass network. The idea beneath this study was to obtain iodine-bearing silver phosphate glasses with a high amount of crosslinking reagents (higher than what could be obtain with alumina in the past [17]) in order to get the highest polymerization degree and, in doing so, an enhanced chemical durability.

2. Materials and Methods

Glasses were prepared using analytical grade AgI (Alfa Aesar, 99.9 %), AgNO₃ (Alfa Aesar, 99.9 %), Nb₂O₅ (Alfa Aesar, 99.5 %), Bi₂O₃ (Aldrich, 99.9 %) and (NH₄)₂HPO₄ (Prolabo, 97.5 %). A two-step synthesis was performed. First, all reagents excepted AgI were heated in a Pt/Au crucible up to 600 °C with a heating rate of 1 °C/min and held for 3 h, in order to remove nitrate, hydroxyl and ammonium groups. The batch was then heated at 900 °C with a heating rate of 5 °C/min and kept at this temperature for 1 h. It was then cast between two brass plates in order to maximize the heat transfer, thus allowing the melt to be cooled at a high speed and limiting the crystallization process. In a second step, iodine-bearing glasses were prepared by grinding the previous glass, mixing it with AgI (weighted to reach 12 wt.% of iodine), and heating the mix at 650 °C for 1 h, which is a sufficient temperature to obtain a melt, which was then cast between two brass plates.

Glass compositions were checked on polished samples by EDS (Bruker AXS X-Flash Detector 4010 system) with standards on a Zeiss SupraTM 55 SEM (Table 1) operating at 15 kV with a probe current of 1 nA. They showed that there was no volatilization of iodine during the

process thanks to the two steps method. The incorporation limit of the crosslinking reagents in presence of iodine was investigated by XRD and by SEM (BSE mode on polished samples). A crosslinking reagent was considered to have reached its incorporation limit when crystallization could be found using either XRD or SEM.

Thermal behavior of the glasses was studied by DSC on ground samples at a heating rate of 10 °C/min, in air and using platinum crucibles.

Structure was investigated by ^{31}P MAS NMR and X-Ray absorption spectroscopy for iodine local environment. ^{31}P MAS NMR spectra were acquired on a 400 MHz (9.4T) Bruker spectrometer with a 4 mm probe, at a spinning speed of 12.5 kHz. For each sample, 8 scans were acquired with a recycling delay of 120 s, and pulse of 2,5 μs and a pulse angle of $\pi/2$. Chemical shift of ^{31}P nuclei are given relative to H_3PO_4 at 0 ppm. We used the conventional notation to describe the connectivity of phosphate units: Q^n_m (n: number of PO_4 units connected to phosphate site; m: number of bismuth or niobium units connected to a phosphate site) [18]. The proportion of Q^n_m units was determined by spectrum simulation with an error of about 5 %.

Iodine K-edge X-Ray absorption spectra were collected on the SAMBA beamline at SOLEIL Synchrotron (proposal 20160062), France. Spectra were collected at 77 K in transmission mode. The X-ray incident energy on the sample was defined using a double-crystal Si (2 2 0) monochromator. The monochromator calibration was performed by collecting the XANES spectrum of a silver foil. The XANES and the EXAFS regions were scanned with 20 eV, 0.08 s. Spectra were collected between 32800 and 34700 eV, setting E_0 at 33172 eV. Depending on the data quality, 30 to 50 XAS data sets were collected per sample and averaged. The data were then processed using the ATHENA package [20]. The EXAFS $\chi(k)$ functions were

weighted by k^2 to enhance oscillations at high k values. The spectra were then Fourier transformed over the k -range $[3-10] \text{ \AA}^{-1}$ using a Hanning apodisation window. Theoretical EXAFS backscattering paths were calculated from the computational modeling. Only simple paths were considered for fitting. The fitting analysis was restrained to the $[1.5-6.0] \text{ \AA}^{-1}$ domain of the radial distribution obtained by the Fourier transform of the EXAFS oscillations. The amplitude factor S_0^2 was set at 0.9 for all shells of all samples.

Finally, information on niobium and bismuth coordination in the glasses was obtained by Raman spectroscopy and X-Ray absorption spectroscopy, respectively. Raman spectra of the AgPO_3 and $\text{AgPO}_3\text{-}2\text{Nb}_2\text{O}_5$ glasses were recorded at room temperature with the 647.1 nm excitation line of a Spectra Physics krypton ion laser. To avoid any degradation of the sample, all the compounds were studied with a very low laser power (3–4 mW at the sample). Four accumulations of a few seconds were used for each spectral range. The beam was focused onto the samples using the macroscopic configuration of the apparatus. No damage of the material by the laser was observed. The scattered light was analyzed with a Raman Dilor XY800 spectrometer equipped with an optical multichannel charge coupled device detector cooled by liquid nitrogen. In the $400\text{--}1300 \text{ cm}^{-1}$ range, the spectral resolution is approximately 0.5 cm^{-1} . The micro-Raman spectrum of the $\text{Ag}_5\text{P}_3\text{O}_{10}\text{-}2\text{Nb}_2\text{O}_5$ glass was recorded at room temperature in the backscattering geometry. The spectral resolution obtained with an excitation source at 532 nm is approximately 1 cm^{-1} . Once again the laser power was kept low ($<10 \text{ mW}$) in order to avoid sample damage. Bismuth L_{III} -edge absorption spectra were collected on the SAMBA beamline at SOLEIL Synchrotron (proposal 20160062), France. Spectra were collected at 77 K in transmission mode. The X-ray incident energy on the sample was defined using a double-crystal Si (2 2 0) monochromator. The monochromator calibration was performed by collecting the XANES spectrum of a silver foil.

The XANES region was scanned with 20 eV, 0.08 s. Spectra were collected between 13100 and 14943 eV, setting E_0 at 13426 eV. Depending on the data quality, 20 to 60 XAS data sets were collected per sample and averaged. The data were then processed using the ATHENA package [20].

Sample name	Theoretical composition (mol%)					Batch (measured) composition (wt.%)					
	AgI	Ag ₂ O	P ₂ O ₅	Nb ₂ O ₅	Bi ₂ O ₃	I (± 1 wt.%)	Ag (± 1 wt.%)	P (± 1 wt.%)	Nb (± 0.1 wt.%)	Bi (± 0.1 wt.%)	O (± 1 wt.%)
Ag ₅ P ₃ O ₁₀	-	62.5	37.5	-	-	-	68.1 (67.7)	11.7 (11.9)	-	-	20.2 (20.4)
AgI- Ag ₅ P ₃ O ₁₀	19.4	50.4	30.2	-	-	12.0 (12.8)	63.2 (61.6)	9.1 (9.2)	-	-	15.7 (16.4)
Ag ₅ P ₃ O ₁₀ - 2Nb ₂ O ₅	-	61.3	36.7	2.0	-	-	66.2 (66.2)	11.4 (11.6)	1.9 (1.5)	-	20.5 (20.7)
AgI- Ag ₅ P ₃ O ₁₀ - 2Nb ₂ O ₅	19.5	49.3	29.6	1.6	-	12.0 (12.7)	61.8 (60.6)	8.9 (9.1)	1.4 (1.0)	-	15.9 (16.6)
Ag ₅ P ₃ O ₁₀ - 3Nb ₂ O ₅	-	60.6	36.4	3.0	-	-	65.4 (66.0)	11.3 (11.7)	2.7 (1.6)	-	20.6 (20.7)
AgI- Ag ₅ P ₃ O ₁₀ - 3Nb ₂ O ₅	19.5	48.8	29.3	2.4	-	12.0 (12.8)	61.1 (60.0)	8.8 (8.9)	2.1 (1.6)	-	16.0 (16.7)
Ag ₅ P ₃ O ₁₀ - 5Nb ₂ O ₅	-	59.4	35.6	5.0	-	-	63.6 (63.7)	11.0 (11.2)	4.6 (4.1)	-	20.8 (21.0)
AgI- Ag ₅ P ₃ O ₁₀ - 5Nb ₂ O ₅	19.7	47.7	28.6	4.0	-	12.0 (*)	59.7 (*)	8.5 (*)	3.6 (*)	-	16.2 (*)
Ag ₅ P ₃ O ₁₀ - 2Bi ₂ O ₃	-	61.2	36.8	-	2.0	-	65.0 (65.0)	11.2 (11.6)	-	4.1 (3.2)	19.7 (20.2)
AgI- Ag ₅ P ₃ O ₁₀ - 2Bi ₂ O ₃	19.8	49.1	29.5	-	1.6	12.0 (11.8)	60.7 (59.9)	8.7 (9.3)	-	3.2 (2.3)	15.4 (16.7)
AgPO ₃	-	50	50	-	-	-	57.7 (56.8)	16.6 (17.0)	-	-	25.7 (26.2)
AgI-AgPO ₃	18.5	40.7	40.7	-	-	12.0 (12.4)	55.1 (55.8)	12.9 (12.1)	-	-	20.0 (19.7)
AgPO ₃ - 2Nb ₂ O ₅	-	49.0	49.0	2.0	-	-	56.1 (56.0)	16.1 (16.5)	2.0 (1.5)	-	25.8 (26.0)
AgI-AgPO ₃ - 2Nb ₂ O ₅	18.6	39.9	39.9	1.6	-	12.0 (12.8)	53.8 (52.6)	12.5 (12.8)	1.5 (1.0)	-	20.2 (20.8)
AgPO ₃ - 3Nb ₂ O ₅	-	48.5	48.5	3.0	-	-	55.3 (54.6)	15.9 (16.5)	2.9 (2.5)	-	25.9 (26.4)
AgI-AgPO ₃ - 3Nb ₂ O ₅	18.7	39.4	39.4	2.4	-	12.0 (13.0)	53.2 (52.2)	12.4 (12.4)	2.3 (1.7)	-	20.1 (20.7)
AgPO ₃ - 2Bi ₂ O ₃	-	49.0	49.0	-	2.0	-	54.9 (54.3)	15.8 (16.2)	-	4.3 (4.0)	25.0 (25.5)
AgI-AgPO ₃ - 2Bi ₂ O ₃	19.0	39.7	39.7	-	1.6	12.0 (12.8)	52.9 (51.7)	12.3 (12.4)	-	3.4 (2.9)	19.4 (20.2)
AgPO ₃ - 3Bi ₂ O ₃	-	48.5	48.5	-	3.0	-	53.6 (53.0)	15.4 (15.9)	-	6.4 (5.9)	24.6 (25.2)
AgI-AgPO ₃ - 3Bi ₂ O ₃	19.2	39.2	39.2	-	2.4	12.0 (12.6)	51.9 (50.6)	12.0 (12.2)	-	5.0 (4.6)	19.1 (20.0)
AgPO ₃ - 5Bi ₂ O ₃	-	47.5	47.5	-	5.0	-	51.0 (51.1)	14.7 (15.0)	-	10.4 (9.8)	23.9 (24.2)
AgI-AgPO ₃ - 5Bi ₂ O ₃	19.6	38.2	38.2	-	4.0	12.0 (13.0)	49.9 (49.5)	11.4 (11.5)	-	8.1 (6.7)	18.6 (19.3)

Table 1. Composition of the studied glasses

((*): The corresponding glass was not obtained and thus no composition was measured)

3. Results

3.1. Incorporation of Nb_2O_5 and Bi_2O_3 in silver phosphate glasses

After XRD analysis and SEM observation (not shown here), no crystallization were detected in phosphate glasses without iodine, whatever the amount of crosslinking reagent (Nb_2O_5 and Bi_2O_3) introduced. According to the definition of the incorporation limit stated above, it can be concluded that without iodine, Nb_2O_5 and Bi_2O_3 are both below their incorporation limit in silver phosphate glasses at the studied concentrations.

Iodine was then added to the previous glasses in the conditions beforehand described. The AgI- $\text{Ag}_5\text{P}_3\text{O}_{10}$ -5 Nb_2O_5 melt was however found to be too viscous at 650 °C to be cast on the brass plates, as the melt did not even flow from the crucible. With no glass available for characterization, the AgI- $\text{Ag}_5\text{P}_3\text{O}_{10}$ -5 Nb_2O_5 composition wasn't further investigated. Despite this limitation is not strictly representative of the incorporation limit as defined above, Nb_2O_5 will be considered to have reached its incorporation limit in the $\text{Ag}_5\text{P}_3\text{O}_{10}$ system in presence of iodine and at this concentration for our synthesis conditions.

Figure 1 shows the XRD patterns of the glasses after iodine addition. Once again, no peak was detected whatever the amount of crosslinking reagent (Nb_2O_5 and Bi_2O_3) introduced. SEM images of the same glasses taken in BSE mode are presented in Figure 2 (for the $\text{Ag}_5\text{P}_3\text{O}_{10}$ system) and Figure 3 (for the AgPO_3 system). For the $\text{Ag}_5\text{P}_3\text{O}_{10}$ set of compositions, no crystallization was found with niobium. However, the addition of iodine in the Bi_2O_3 -containing glass induced the expulsion of some of the bismuth from the glass matrix and the subsequent formation of BiPO_4 crystallizations (composition calculated by EDS analysis). The same phenomenon can be observed in the AgPO_3 set of compositions with both Nb_2O_5

(leading to the formation of a non-identified niobio-phosphate phase for the $\text{AgI-AgPO}_3\text{-}3\text{Nb}_2\text{O}_5$ glass) and Bi_2O_3 (leading once again to the formation of BiPO_4 , but this time for the $\text{AgI-AgPO}_3\text{-}5\text{Bi}_2\text{O}_3$ glass).

The fact that these crystallizations were not detected using XRD can be explained by a low concentration in the glasses. It is however enough to state that the crosslinking reagents have reached their incorporation limits in the iodine silver phosphate glasses at these concentrations. Table 2 displays a summary of these results by presenting the maximum Nb_2O_5 and Bi_2O_3 concentrations that can be introduced in iodine-containing silver phosphate glasses to obtain glasses with no crystallization, depending on the Ag/P ratio of the glasses and in the conditions of our tests (addition of 12 wt.% of iodine to a glass frit at 650 °C).

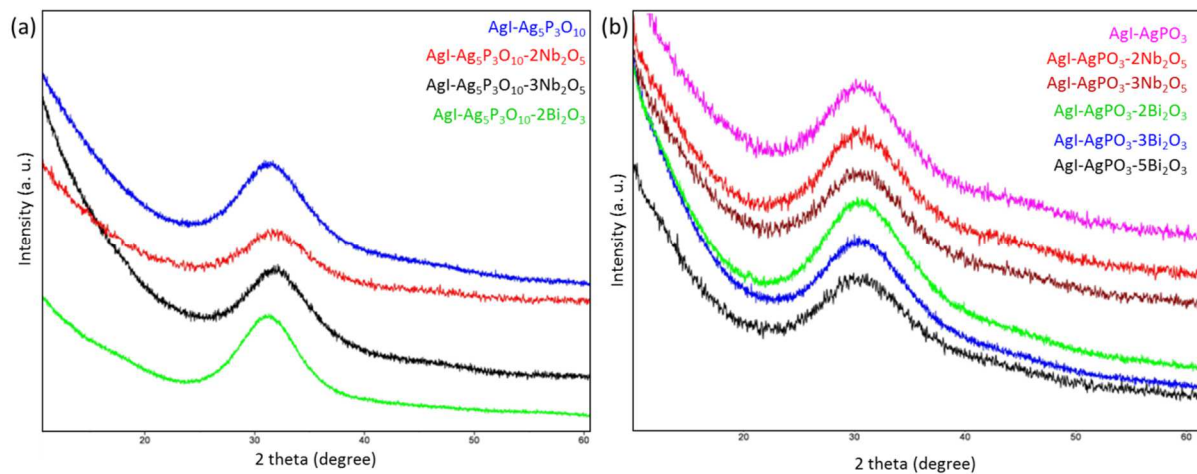


Figure 1. XRD patterns of glasses in the $\text{Ag}_5\text{P}_3\text{O}_{10}$ (a) and AgPO_3 (b) systems after iodine addition.

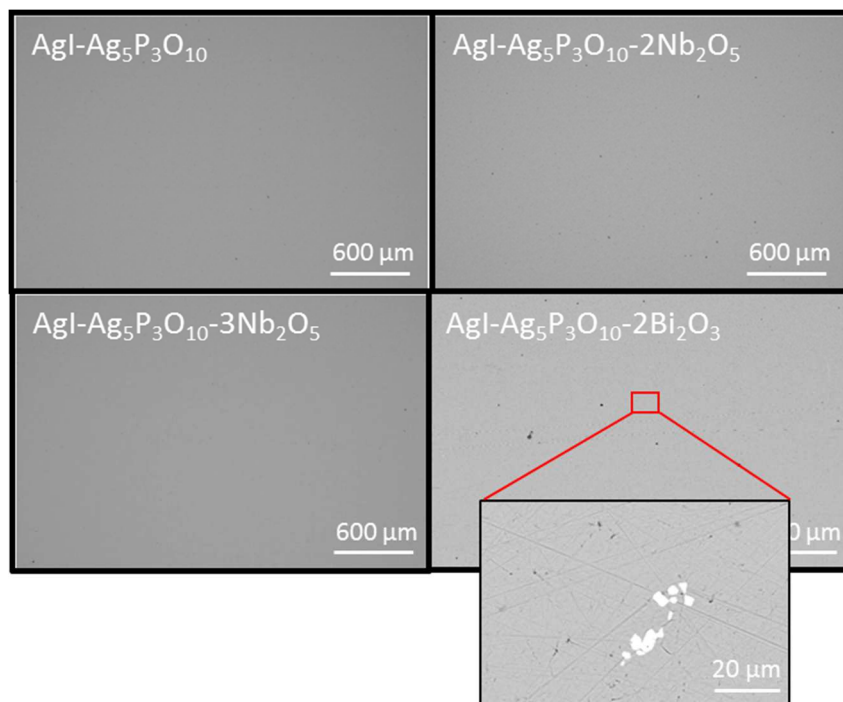


Figure 2. SEM images (BSE mode) of glasses in the $\text{Ag}_5\text{P}_3\text{O}_{10}$ system after iodine addition.

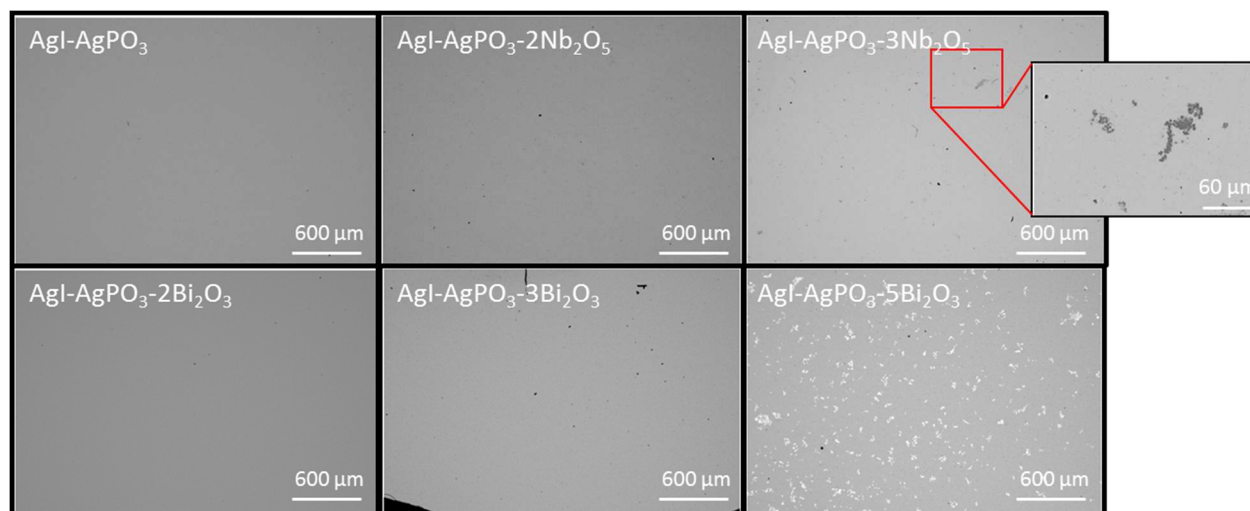


Figure 3. SEM images (BSE mode) of glasses in the AgPO_3 system after iodine addition.

System	Maximum crosslinking reagent concentration in presence of iodine (mol%) <i>(measured experimentally)</i>	
	Nb ₂ O ₅	Bi ₂ O ₃
AgPO ₃	1.6 <i>(1.0)</i>	2.4 <i>(2.0)</i>
Ag ₅ P ₃ O ₁₀	2.4 <i>(1.8)</i>	< 1.6 <i>(< 1.1)</i>

Table 2. Maximum Nb₂O₅ and Bi₂O₃ concentrations in silver phosphate glasses in presence of iodine (12 wt.%) to obtain a glass with no crystallization.

3.2. Glass transition temperature

The evolution of the glass transition temperature (T_g) of the glasses depending on the amount of crosslinking reagent is presented Figure 4 for the Ag₅P₃O₁₀ set of compositions, and Figure 5 for the AgPO₃ set of compositions. In each case, it can be noticed that the addition of a crosslinking reagent to a glass without iodine induces a steady increase of T_g , meaning that they have a visible effect on the glass network polymerization, even at low concentration. Then, the addition of iodine to these glasses leads to an important drop of T_g as it has already been observed [14-15]. However, in presence of iodine, even if the T_g of the crosslinking reagent-containing glasses is slightly higher than those of glasses without any crosslinking reagent, it can also be noticed that the increase of the crosslinking reagent concentration in these glasses doesn't impact the T_g . Indeed, whatever the content of Bi₂O₃ or Nb₂O₅, in presence of iodine, the glass transition temperature is of about 139 °C (\pm 5 °C) for the Ag₅P₃O₁₀ set of compositions, and of about 162 °C (\pm 5 °C) for the AgPO₃ set of compositions.

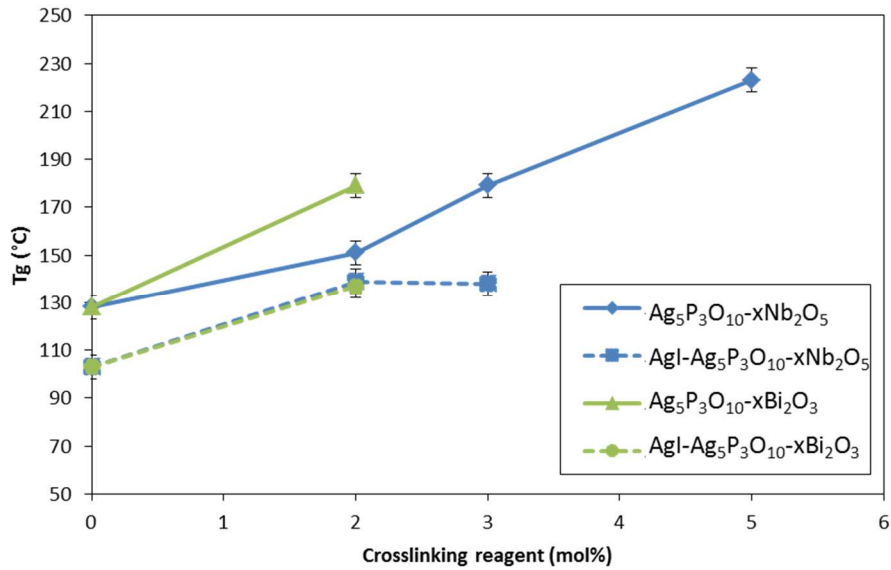


Figure 4. Evolution of the glass transition temperature (T_g) versus the content of crosslinking reagent for glasses of the $Ag_5P_3O_{10}$ set.

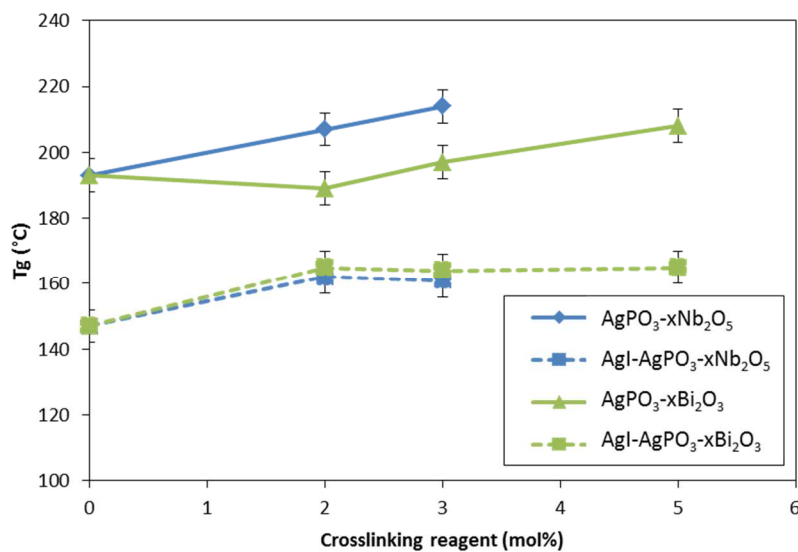


Figure 5. Evolution of the glass transition temperature (T_g) versus the content of crosslinking reagent for glasses of the $AgPO_3$ set.

Moreover, it seems that Nb_2O_5 and Bi_2O_3 don't affect the T_g of the non-iodine containing glasses with the same intensity. Indeed, for $Ag_5P_3O_{10}$ system, the addition of 2 mol% of Bi_2O_3 induces a higher increase of the T_g than the addition of 2 mol% of Nb_2O_5 , while it is the opposite for $AgPO_3$ system. However, bismuth and niobium should not be compared based on their molar amount. Indeed, as their charges are different, they don't bring the same

number of oxygen in the glass, and thus the polymerization gained from a same molar amount is different. Instead, their effect should be compared depending on the number of oxygens brought in the glass network. Figure 6 shows the evolution of the glass transition temperature depending on the number of oxygen brought by the crosslinking reagents for the non-iodine containing glasses. When taking this parameter into consideration, it can be noticed that Nb_2O_5 and Bi_2O_3 affect the T_g from the AgPO_3 set of compositions with almost the same intensity. Considering the $\text{Ag}_5\text{P}_3\text{O}_{10}$ set of compositions however, it can be noticed that the bismuth has a significantly higher impact on the glass transition temperature. Thus it seems that Bi_2O_3 is a more efficient crosslinking reagent than Nb_2O_5 . The fact that this difference in efficiency is not observed for the AgPO_3 set of compositions could be explained by the fact that the $\text{Ag}_5\text{P}_3\text{O}_{10}$ system is more depolymerized from the start, thus giving the crosslinking reagents more leeway to polymerize the glass network. This seems to be confirmed by the fact that in the $\text{Ag}_5\text{P}_3\text{O}_{10}$ system, the addition of the crosslinking reagent induces an increase of up to 100 °C, while this increase is limited to about 30 °C for the AgPO_3 system. The fact that AgPO_3 is more polymerized than $\text{Ag}_5\text{P}_3\text{O}_{10}$ from the start would then reduce the difference of efficiency between Nb_2O_5 and Bi_2O_3 .

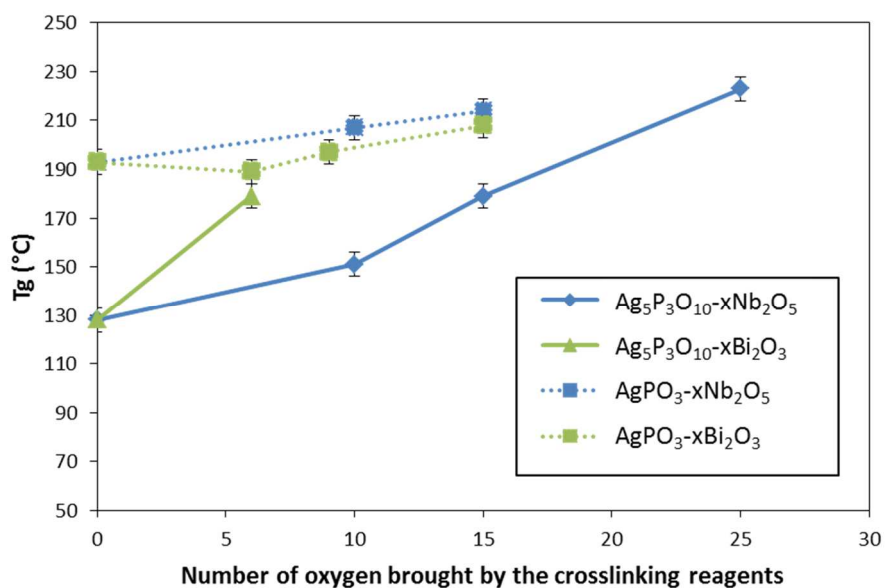
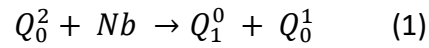


Figure 6. Evolution of the glass transition temperature (T_g) versus on the number of oxygens brought by the crosslinking reagents for the non-iodine containing glasses.

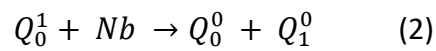
3.3. Structure of the glasses

^{31}P MAS NMR

The ^{31}P MAS NMR spectra of the glasses from the $Ag_5P_3O_{10-x}Nb_2O_5$ set of compositions with and without iodine are shown on Figure 7. The proportion of Q^n_m groups has been calculated by spectrum simulation and is reported in Table 3. As expected, the $Ag_5P_3O_{10}$ spectrum displays two resonances at 7 ppm and at -15 ppm, attributed to Q^1_0 and Q^2_0 groups, respectively. The addition of Nb_2O_5 to this composition induces a decrease in the proportion of Q^1_0 and Q^2_0 groups, which are replaced by Q^1_1 groups (resonance at -3 ppm), representative of the creation of P-O-Nb-O-P bonds in the glass network. It also induces the apparition of two resonances at 28 ppm and 16 ppm, attributed to Q^0_0 and Q^0_1 units, respectively. While the proportion of Q^0_1 units is really low for the $Ag_5P_3O_{10-2}Nb_2O_5$ and $Ag_5P_3O_{10-3}Nb_2O_5$ glasses ($\sim 1\%$), it is significant for the $Ag_5P_3O_{10-5}Nb_2O_5$ glass, which displays up to 8.7 % of Q^0_1 units. The presence of these units can be explained by a depolymerization of the glass network with the addition of niobium:



This reorganization also explains the brutal decrease of Q_0^2 units and the increase of Q_0^1 units that can be observed for the $Ag_5P_3O_{10}-5Nb_2O_5$ glass. Concerning the Q_0^0 units, they can be seen only for the $Ag_5P_3O_{10}-5Nb_2O_5$ glass and only at a very low amount (< 0.1 %). Their presence can also be explained by a depolymerization of the glass network with the addition of niobium:



The addition of iodine to these glasses is followed by a shift of the chemical shift of each resonance by a few ppm toward more negative values. This was explained by an increase of bond lengths and bond angles induced by the introduction of large iodine anions in the glass [16]. However, this has no effect on the evolution of the proportion of Q_m^n units depending on the amount of niobium, which is the same as for the glasses containing no iodine (see Table 3), excepted for the $AgI-Ag_5P_3O_{10}-2Nb_2O_5$ glass, which displays an unexpectedly high amount of Q_0^1 units.

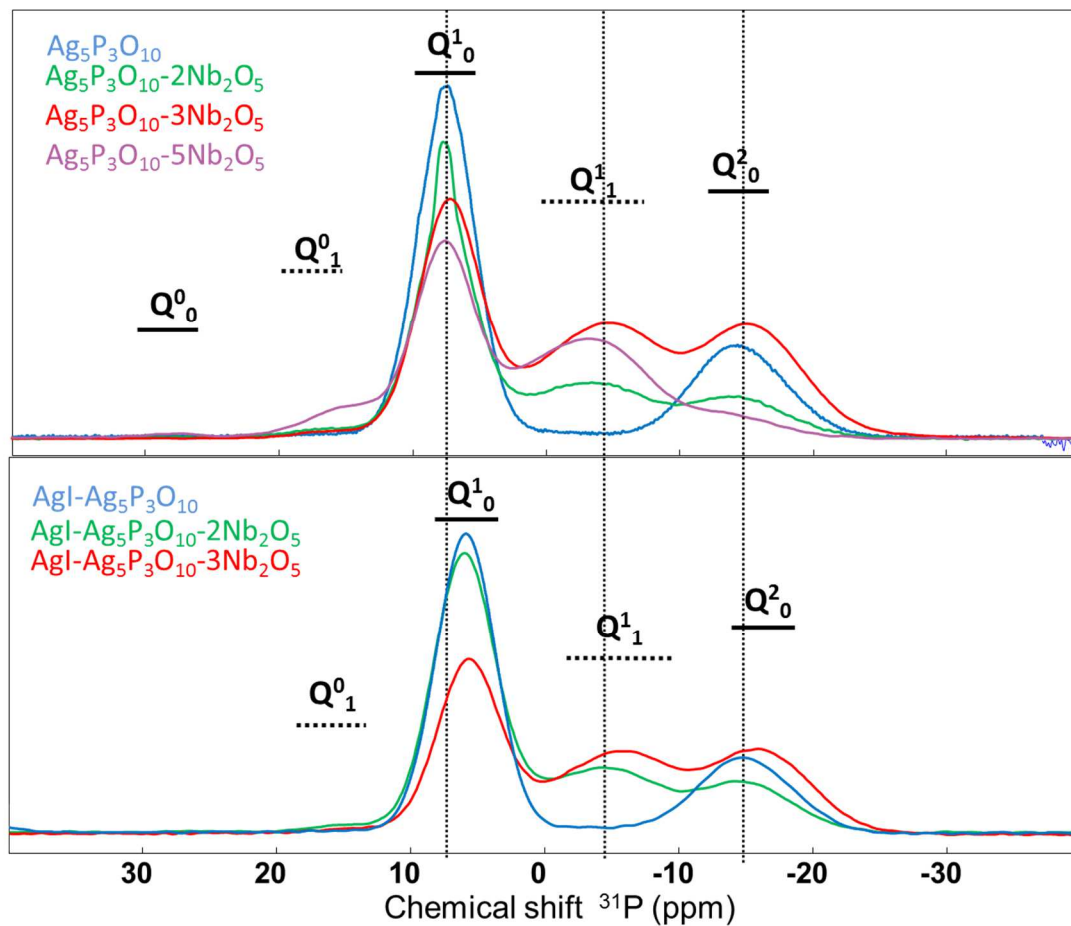
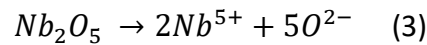


Figure 7. ^{31}P MAS NMR spectra of the glasses from the $\text{Ag}_5\text{P}_3\text{O}_{10-x}\text{Nb}_2\text{O}_5$ set of compositions without (top) and with (bottom) AgI.

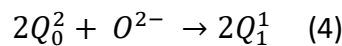
δ (ppm)	Q^0_0 28 ppm	Q^0_1 16 ppm	Q^1_0 7 ppm	Q^1_1 -3 ppm	Q^2_0 -15 ppm
$\text{Ag}_5\text{P}_3\text{O}_{10}$	-	-	69.6 %	-	30.4 %
$\text{Ag}_5\text{P}_3\text{O}_{10-2}\text{Nb}_2\text{O}_5$	-	1.2 %	39.7 %	30.2 %	28.7 %
$\text{Ag}_5\text{P}_3\text{O}_{10-3}\text{Nb}_2\text{O}_5$	-	0.7 %	36.5 %	36.5 %	26.3 %
$\text{Ag}_5\text{P}_3\text{O}_{10-5}\text{Nb}_2\text{O}_5$	< 0.1 %	8.7 %	43.5 %	42.2 %	5.6 %
δ (ppm)	-	Q^0_1 15 ppm	Q^1_0 5 ppm	Q^1_1 -5 ppm	Q^2_0 -16 ppm
$\text{AgI-Ag}_5\text{P}_3\text{O}_{10}$	-	-	68.9 %	-	31.1 %
$\text{AgI-Ag}_5\text{P}_3\text{O}_{10-2}\text{Nb}_2\text{O}_5$	-	< 0.1 %	61.2 %	24.6 %	14.2 %
$\text{AgI-Ag}_5\text{P}_3\text{O}_{10-3}\text{Nb}_2\text{O}_5$	-	< 0.1 %	39.0 %	38.0 %	23.0 %

Table 3. Proportion of Q^n_m groups for the glasses from the $\text{Ag}_5\text{P}_3\text{O}_{10-x}\text{Nb}_2\text{O}_5$ set of compositions with (top) and without (bottom) AgI.

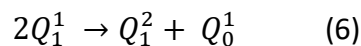
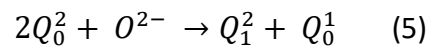
The ^{31}P MAS NMR spectra of the glasses from the $\text{AgPO}_3\text{-xNb}_2\text{O}_5$ set of compositions (with and without iodine) are shown on Figure 8. The proportion of Q^n_m groups has been calculated by spectrum simulation and is reported in Table 4. The AgPO_3 spectrum displays a main resonance at -17 ppm, which can be assigned to Q^2_0 groups. Then, the addition of Nb_2O_5 induces a decrease of the proportion of Q^2_0 groups and the apparition of Q^1_0 groups (at 7 ppm), Q^1_1 groups (at -6 ppm) and of Q^2_1 groups (at -28 ppm). Q^1_1 and Q^2_1 groups result from the creation of new bonds in the glass network, which were expected with the addition of niobium. The appearance of Q^1_0 groups is more surprising but can be easily explained. Indeed, the addition of a crosslinking reagent (here Nb_2O_5) can manifest itself as two reactions. The first one is the reaction of Nb_2O_5 dissociation, which can be written as follows:



The second reaction is the reaction of the glass network depolymerization, which can be written as follows:



Finally, the appearance of Q^1_0 groups can be explained by a reorganization of charges, which can be described by the two following reactions [16]:



The addition of iodine to these glasses is here again followed by a shift of the chemical shift of each resonance by a few ppm, without incidence on the proportion of Q^n_m groups. Finally, it can be noted that the AgPO_3 and the AgI-AgPO_3 glasses both display a very small amount

of Q^1_1 units, which should not exist considering the absence of a crosslinking reagent. This could be explained by the presence of some hydroxyls groups during the synthesis of these glasses. Indeed, *Wenslow and Mueller* [21] reported a resonance at -5.8 ppm in sodium metaphosphate glasses, which was attributed to a Q^1_{1H} unit.

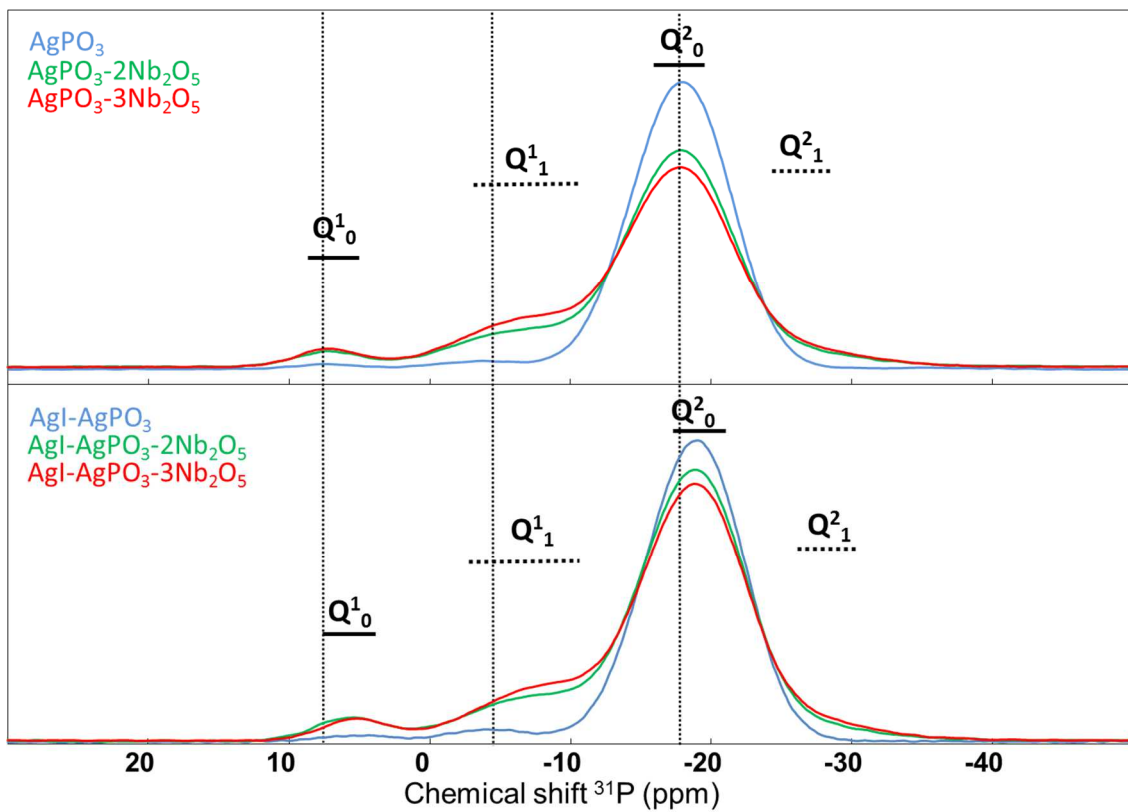


Figure 8. ^{31}P MAS NMR spectra of the glasses from the $\text{AgPO}_3\text{-xNb}_2\text{O}_5$ set of compositions without (top) and with (bottom) AgI.

δ (ppm)	Q ¹ ₀ 7 ppm	Q ¹ ₁ -6 ppm	Q ² ₀ -17 ppm	Q ² ₁ -28 ppm
AgPO ₃	0.6 %	3.9 %	95.5 %	-
AgPO ₃ -2Nb ₂ O ₅	3.2 %	15.1 %	79.4 %	2.4 %
AgPO ₃ -3Nb ₂ O ₅	2.9 %	19.1 %	73.5 %	4.4 %
δ (ppm)	Q ¹ ₀ 5 ppm	Q ¹ ₁ -7 ppm	Q ² ₀ -19 ppm	Q ² ₁ -30 ppm
AgI-AgPO ₃	0.6 %	0.8 %	98.5 %	-
AgI-AgPO ₃ -2Nb ₂ O ₅	5.0 %	10.8 %	83.3 %	0.9 %
AgI-AgPO ₃ -3Nb ₂ O ₅	3.6 %	18.2 %	73.0 %	5.1 %

Table 4. Proportion of Qⁿ_m groups for the glasses from the AgPO₃-xNb₂O₅ set of compositions with (top) and without (bottom) AgI.

The ³¹P MAS NMR spectra of the glasses from the AgPO₃-xBi₂O₃ set of compositions (with and without iodine) are shown on Figure 9. The proportion of Qⁿ_m groups has been calculated by spectrum simulation and is reported in Table 5. Like with Nb₂O₅, the addition of Bi₂O₃ to the silver phosphate glass induces a decrease of the proportion of Q²₀ groups and the apparition of Q¹₀ groups (at 7 ppm), Q¹₁ groups (at -2 ppm) and of Q²₁ groups (at -28 ppm). Once again, Q¹₁ and Q²₁ groups result from the creation of new bonds in the glass network, which were expected with the addition of bismuth, while the Q¹₀ groups can be explained by the same reactions as those described previously. Finally, it can also be noticed that here again the addition of iodine induces a shift of chemical shift of each resonance by a few ppm with no incidence on the proportion of Qⁿ_m groups.

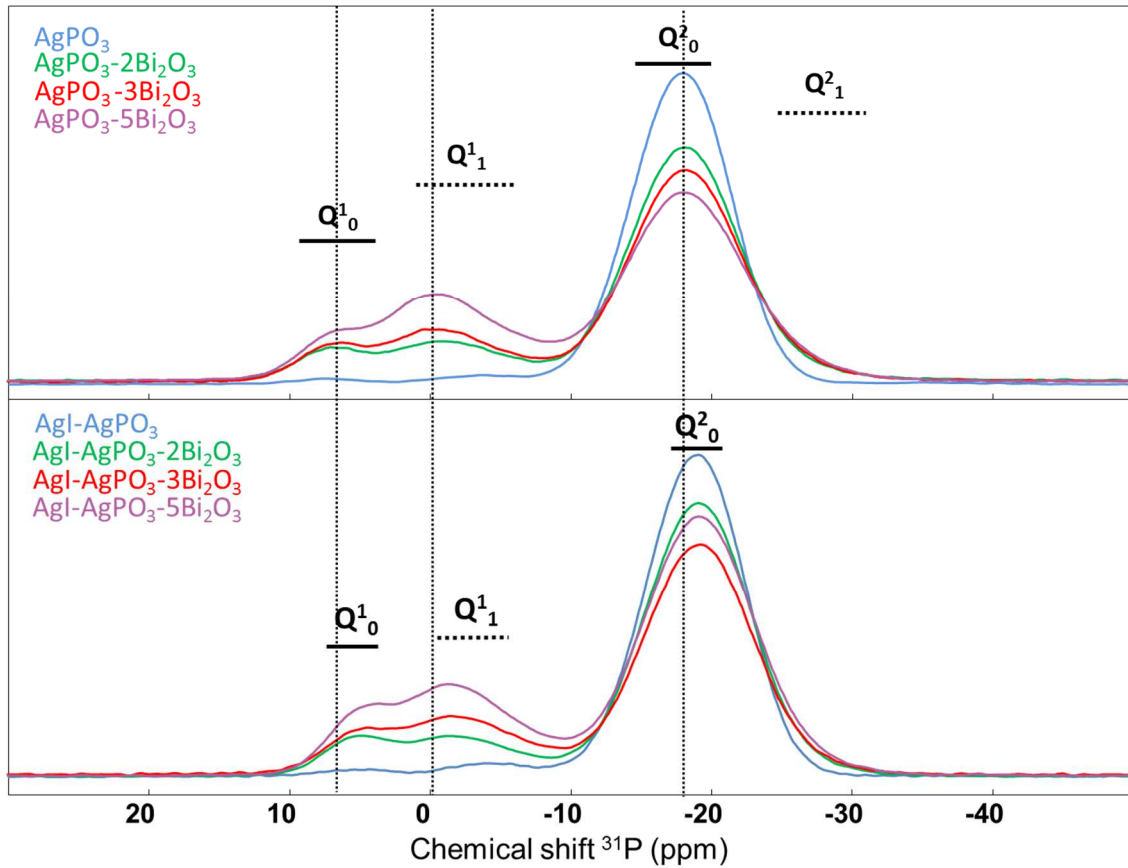


Figure 9. ^{31}P MAS NMR spectra of the glasses from the $\text{AgPO}_3\text{-xBi}_2\text{O}_3$ set of compositions without (top) and with (bottom) AgI.

δ (ppm)	Q^1_0	Q^1_1	Q^2_0	Q^2_1
	7 ppm	-2 ppm	-18 ppm	-28 ppm
AgPO ₃	0.6 %	3.9 %	95.5 %	-
AgPO ₃ -2Bi ₂ O ₃	5.6 %	13.5 %	79.4 %	1.6 %
AgPO ₃ -3Bi ₂ O ₃	3.6 %	20.4 %	73.0 %	2.9 %
AgPO ₃ -5Bi ₂ O ₃	3.8 %	31.8 %	63.7 %	0.6 %
δ (ppm)	Q^1_0	Q^1_1	Q^2_0	Q^2_1
	5 ppm	-4 ppm	-19 ppm	-29 ppm
AgI-AgPO ₃	0.6 %	0.8 %	98.5 %	-
AgI-AgPO ₃ -2Bi ₂ O ₃	5.4 %	13.6 %	80.0 %	0.8 %
AgI-AgPO ₃ -3Bi ₂ O ₃	5.3 %	24.4 %	69.9 %	0.7 %
AgI-AgPO ₃ -5Bi ₂ O ₃	5.5 %	26.8 %	67.1 %	0.7 %

Table 5. Proportion of Q^n_m groups for the glasses from the $\text{AgPO}_3\text{-xBi}_2\text{O}_3$ set of compositions with (top) and without (bottom) AgI.

Iodine environment

Iodine K-edge X-Ray absorption spectra for crystalline β -AgI, AgI-AgPO₃ glass and AgI-AgPO₃-5Bi₂O₃ glass are shown on Figure 10. Parameters extracted from the fitting of these spectra are reported in Table 6. Firstly, it can be noticed that the introduction of bismuth in the glass has no effect on the iodine local environment, as the spectra for AgI-AgPO₃ and AgI-AgPO₃-5Bi₂O₃ glasses are perfectly stackable. This is confirmed by the fitting parameters that are identical. It can also be seen that in these two glasses, the local structure around iodine is very similar to that found in crystalline silver iodide. In the present glasses iodine is found to be surrounded by 4 silver atoms, forming a slightly deformed tetrahedron (as one Ag atom is at 3.05 Å while the other 3 are at 2.79 Å), which presents dimensions similar to crystalline AgI ($d_{\text{I-Ag}} = 2.81$ Å). Finally, while the second sphere of coordination can easily be observed for AgI (with 12 iodine atoms at 4.58 Å), it is not observed for the two glasses, meaning that no crystalline clusters are formed and that silver iodide is well dispersed in the network.

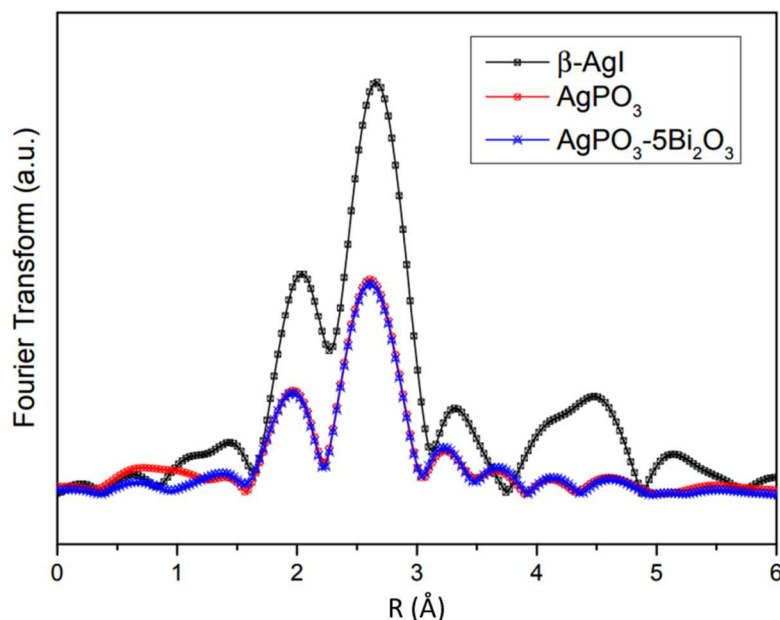


Figure 10. Radial distribution function (RDF) for iodine K-edge EXAFS spectra recorded from β -AgI, AgI-AgPO₃ glass and AgI-AgPO₃-5Bi₂O₃ glass.

Sample	Atom (X)	N _{l-x}	d _{l-x} (Å)	σ ²	R-factor
β-Agl (crystal)	Ag	4	2.81	0.01	0.002
	I	12	4.58	0.02	
Agl-AgPO ₃	Ag	3	2.79	0.01	0.008
	Ag	1	3.05	0.01	
Agl-AgPO ₃ -5Bi ₂ O ₃	Ag	3	2.79	0.01	0.009
	Ag	1	3.05	0.01	

Table 6. Fitting parameters obtained for iodine K-edge EXAFS spectra recorded from β-Agl, AgI-AgPO₃ glass and AgI-AgPO₃-5Bi₂O₃ glass.

Nb and Bi coordination

Raman spectra of AgPO₃, AgPO₃-2Nb₂O₅ and Ag₅P₃O₁₀-2Nb₂O₅ are shown on Figure 11. The niobium-containing glasses both show a clear band at 880 cm⁻¹ and 910 cm⁻¹ for AgPO₃ and Ag₅P₃O₁₀, respectively. This band, which does not appear on the AgPO₃ glass, has already been observed in silver-doped niobio-phosphate glasses [22] as well as other niobio-phosphate glasses [23-24] and is attributed to the stretching vibration of the Nb-O short bond in the isolated and distorted NbO₆ octahedra.

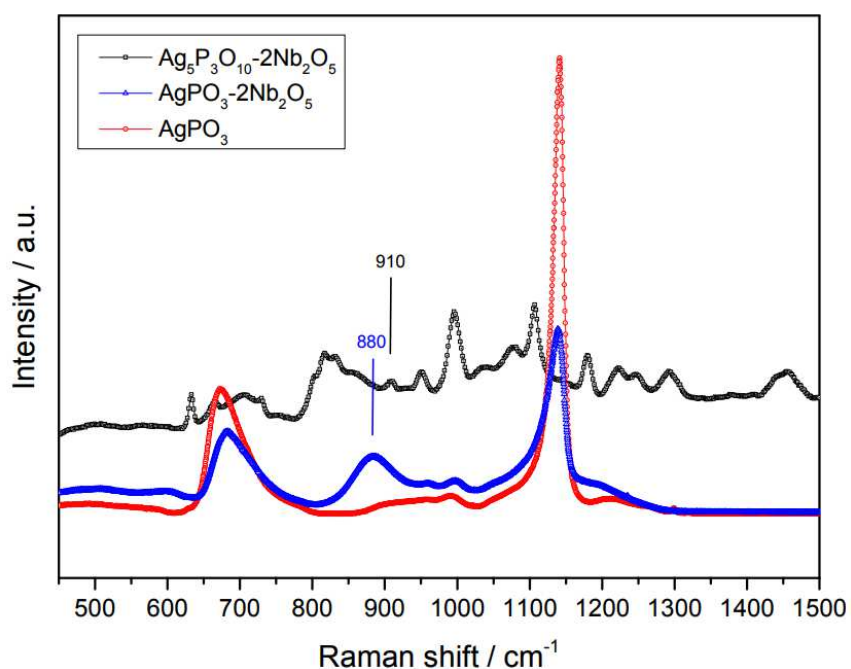


Figure 11. Raman spectra of the AgPO₃, AgPO₃-2Nb₂O₅ and Ag₅P₃O₁₀-2Nb₂O₅, glasses.

Figure 12 shows the Bi L_{III}-edge XABES spectra of the AgI-AgPO₃-5Bi₂O₃ glass, as well as two crystalline references: Bi₂O₃ and Na₃Bi(PO₄)₂. Data shown for the Na₃Bi(PO₄)₂ are courtesy of

Daviero *et al.* [25]. The comparison of these three spectra reveals that Bi local environment in the glass is closer to $\text{Na}_3\text{Bi}(\text{PO}_4)_2$ than to Bi_2O_3 . In the former the bismuth cation is in an octahedral coordination, surrounded by 8 oxygen atoms. This octahedron is however distorted, due to the presence of the $6s^2$ electronic lone pair. Bi is thus surrounded by a first shell of 5 oxygen atoms, and a second shell of 3 oxygen atoms [25].

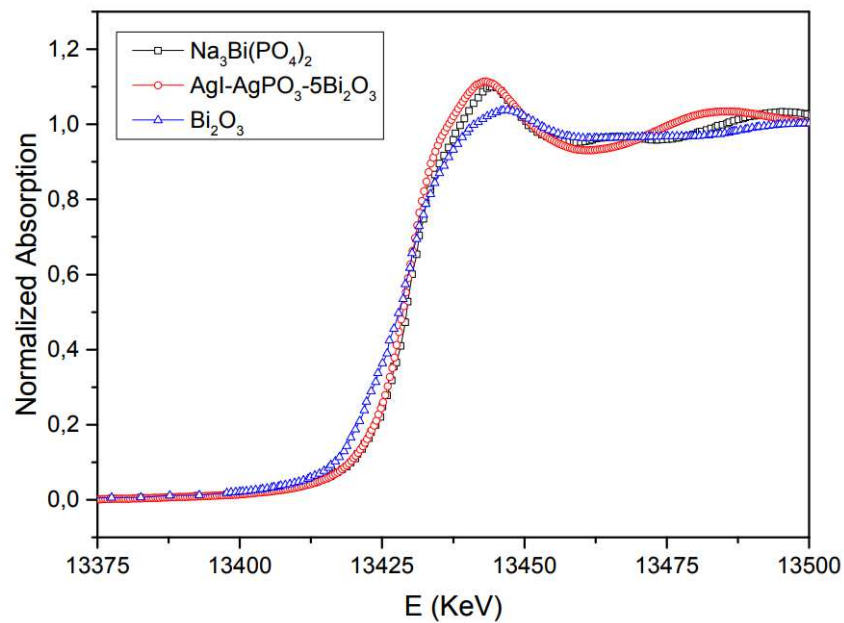


Figure 12. Bi L_{III} -edge XANES spectra of $\text{Na}_3\text{Bi}(\text{PO}_4)_2$, $\text{AgI-AgPO}_3\text{-}85\text{Bi}_2\text{O}_3$ glass and Bi_2O_3 .

4. Discussion

4.1. Valence units theory

Brow *et al.* [26] have previously used valence units (VU) to describe the bond characteristics after the incorporation of alumina in phosphate glasses. A bond valence unit (VU) is defined as the charge divided by the coordination number of the considered atom. The most favorable structures are those for which the nearest neighbors of oxygen contribute to form bonds with a total charge of +2. Figure 13 shows the number of available valence units for Q^0 , Q^1 and Q^2 units in phosphate glasses. Depending on the number of bonding oxygens, the

crosslinking reagent (M^{+6}) will have to bring 0.75 vu (Q^0 units), 0.66 vu (Q^1 units) or 0.5 vu (Q^2 units) for the bond to be stable.

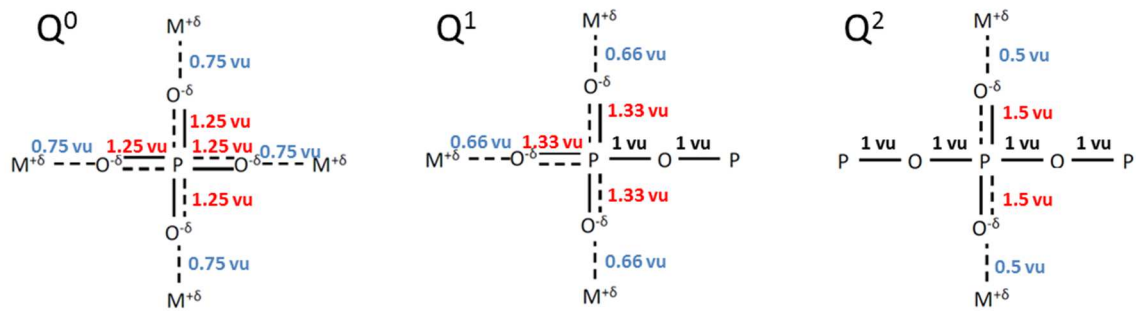


Figure 13. Valence units available depending on the number of bridging oxygens in phosphate glasses [17].

Table 7 shows the number of valence units available for aluminum, niobium and bismuth, depending on their coordination in the glass network. For Al^{3+} , both tetrahedral and octahedral coordination are possible considering the number of valence units. However, previous works [16] showed that for the Ag/P ratio considered here, aluminum was predominantly in octahedral coordination ($Al(6)$). For Bi^{3+} , only the pyramidal ($Bi(3)$) and the octahedral ($Bi(6)$) coordinations are reported in literature [27-28]. Moreover, XANES data acquired for the $AgI-AgPO_3-5Bi_2O_3$ glass show that bismuth coordination in this glass is octahedral (Figure 11). Thus it can be considered that this coordination is most likely to be found in the others glasses.

	Coordination 3	Coordination 4	Coordination 6
Al^{3+}	-	0.75 vu	0.5 vu
Nb^{5+}	-	1.25 vu	0.83 vu
Bi^{3+}	1 vu	-	0.5 vu

Table 7. Valence units available for Al^{3+} , Nb^{5+} and Bi^{3+} depending on their coordination.

For Nb^{5+} , both the tetrahedral ($Nb(4)$) and octahedral ($Nb(6)$) coordinations can be found in the literature [23-24]. Once again, experimental data obtained from Raman analysis show

that niobium is in the octahedral coordination (Figure 10). For this coordination, it can be noticed that the number of valence units available is higher than those available from phosphate groups. Considering the phosphate groups, the bond will be the most stable with the Q^0 ones, as the charge of this bond will be the closest to +2.

Taking that into account these considerations, Nb_2O_5 can be expected to form more bonds in a glass with a high Ag/P ratio, since those glasses display a higher content of Q^0 units to which niobium will be bound. On the contrary, Bi_2O_3 can be expected to form more bonds in a glass with a lower Ag/P ratio, since it will be easier for it to bond with Q^2 units. In particular, this can explain that Nb_2O_5 seems to have a higher incorporation limit in $Ag_5P_3O_5$ glasses (Ag/P = 1.66) than in $AgPO_3$ glasses (Ag/P = 1), and that it seems to be the contrary for Bi_2O_3 .

4.2. Dissociation of crosslinking reagents in silver phosphate glasses

^{31}P NMR can also give information about the incorporation of the crosslinking reagents in the glass network. Actually, the incorporation of a given crosslinking reagent does not mean that it fully contributes to the creation of new bonds with phosphate groups in the glass network, as it can remain partially connected through M-O-M bonds. To make sure of that, the proportion of Q^1 and Q^2 groups to be expected (considering a full dissociation of Nb_2O_5 or Bi_2O_3) needs to be calculated and compared to the experimental values. Considering a binary distribution of Q^n species [29], the equations for calculating the proportions $f(Q^1)$ and $f(Q^2)$ of Q^1 and Q^2 groups, respectively, are the following:

$$f(Q^1) = \frac{3.5 - O/P}{0.5} \times 100 \quad (7)$$

$$f(Q^2) = 100 - f(Q^1) \quad (8)$$

The ratio O/P is obtained from experimental values in Table 1. Experimental proportions $f(Q^n)$ have been calculated as follow :

$$f(Q^1) = f(Q_0^1) + f(Q_1^1) \quad (9)$$

$$f(Q^2) = f(Q_0^2) + f(Q_1^2) \quad (10)$$

The comparison between calculated and experimental fractions of Q^n units for niobium-containing glasses is shown on Figure 14 and Figure 15 for the $Ag_5P_3O_{10}$ and $AgPO_3$ systems, respectively. In both cases it can be noticed that the calculated and the experimental values are close up to a certain amount of Nb_2O_5 . Indeed, at 5 mol% of Nb_2O_5 in the $Ag_5P_3O_{10}$ glass and at 3 mol% of Nb_2O_5 in the $AgPO_3$ glass, the experimental values deviate from the calculated ones. In the case of the $Ag_5P_3O_{10}$ glass with 5 mol% Nb_2O_5 , the experimental number of Q^2 units is lower than the expected one, while the calculated and experimental numbers of Q^1 units are identical. The compensation is done by the appearance of Q_1^0 units (8.7 %), as expected from the valence units discussion above, which are not taken into account in the calculated fractions but which are clearly seen on the spectrum. Thus it can be concluded that Nb_2O_5 is fully dissociated in the $Ag_5P_3O_{10}$ glasses. However, in the case of the $AgPO_3$ glass with 3 mol% Nb_2O_5 , the number of Q^2 units is higher than the calculated one, while the number of Q^1 units is lower. In this case, it can be concluded that the dissociation of Nb_2O_5 is not complete. Therefore, only a part of the niobium contributes to the creation of new bonds in the network and another part constitutes an O-Nb-O-Nb-O sub-network.

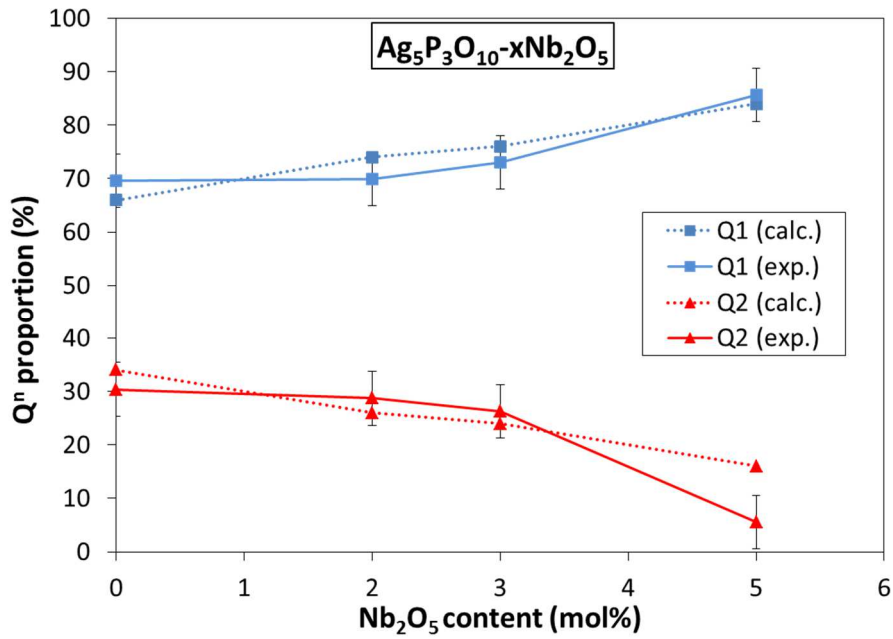


Figure 14. Comparative evolution of Qⁿ proportions obtained by calculation (calc.) and from experimental spectra (exp.) for Ag₅P₃O_{10-x}Nb₂O₅ glasses.

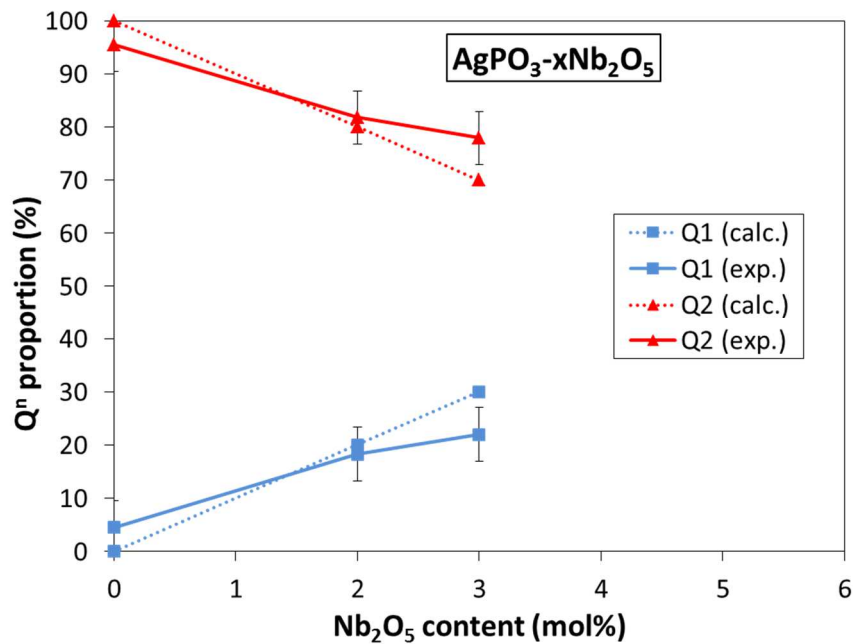


Figure 15. Comparative evolution of Qⁿ proportions obtained by calculation (calc.) and from experimental spectra (exp.) for AgPO_{3-x}Nb₂O₅ glasses.

The comparison between calculated and experimental fractions of Qⁿ units for bismuth-containing glasses is shown on Figure 16 (AgPO₃ system). Once again, there is a difference between the experimental and the calculated values of Qⁿ units in these glasses. However, this difference can be observed from the first glass (without bismuth) and is constant with

the increase of the Bi_2O_3 content. It can be explained by the presence of a high amount of hydroxyl groups; which were observed in the AgPO_3 glass. The fact that these groups have an impact on the $\text{AgPO}_3\text{-xBi}_2\text{O}_3$ system and not on the $\text{AgPO}_3\text{-xNb}_2\text{O}_5$ system can be explained by the fact that Nb_2O_5 have a higher crosslinking power, but also by the fact that Nb_2O_5 is not fully dissociated in the AgPO_3 system, thus masking the effect of those hydroxyl groups. Concerning the dissociation of Bi_2O_3 , considering that the experimental fraction of Q^2 units is lower than expected, and that the difference between theoretical and experimental values is due to hydroxyls groups, it can be concluded that Bi_2O_3 is fully dissociated in these glasses. As such, all the introduced bismuth contributes to the creation of new bonds in the glass network.

It must be noted that the discussion is based on glasses without iodine. Still, it is the same for iodine-containing glasses, as we have shown (Figure 8) that the addition of silver iodide does not significantly change the repartition of Q^n units.

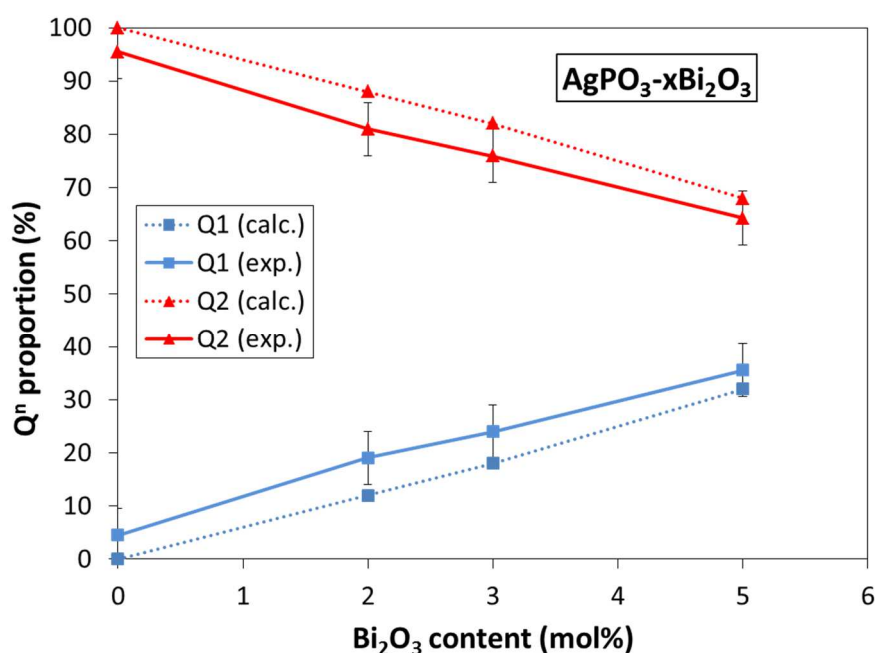


Figure 16. Comparative evolution of Q^n proportions obtained by calculation (calc.) and from experimental spectra (exp.) for $\text{AgPO}_3\text{-xBi}_2\text{O}_3$ glasses.

4.3. Effect of crosslinking reagent on the glass properties

³¹P MAS NMR has shown that the addition of niobium and bismuth oxides does have a significant effect on the glass structure, as it contributes to the creation of new bonds in the glass network and thus increases the polymerization degree of the glasses. Consequently, this modification of the glass structure has also an impact on the glass properties, which is illustrated by the increase of the glass transition temperature as seen on Figures 4 and 5 (at least for glasses containing no iodine). For these glasses, we have shown that the addition of a crosslinking oxide has had the expected effect on the glass properties.

After addition of silver iodide however, while the NMR experiments show no decrease of the polymerization degree, there is a significant drop of the T_g . Previous works [16, 30] attributed this drop to a decrease of the electrostatic forces between the phosphate groups, which is caused by the introduction of large AgI entities. While this addition has no effect on the polymerization degree of the glass, it has an effect on the geometry of PO₄ tetrahedra, as it is followed by an increase of the Ag-O bond lengths [30], leading to a weakening of the network, and thus a decrease of glass transition temperature.

It can also be noticed that for iodine-containing glasses, the effect of the crosslinking reagents on the T_g is limited. Indeed, while glasses containing a crosslinking reagent show higher glass transition temperatures than those without crosslinking reagent, it can also be pointed out that whatever the amount of crosslinking reagent added, the T_g were identical after AgI addition. This seems to be in contradiction with the results obtained from ³¹P MAS NMR, which show that the polymerization degree of the glasses increases with the amount of crosslinking reagent even for iodine-bearing glasses. Consequently, it will be interesting to

see if this limited effect on thermal properties is also reflected on the chemical durability properties of these glasses. We will report a detailed study of the chemical durability in a forthcoming paper, which will consider both short and long term stability under several alteration conditions.

5. Conclusion

Silver-phosphate glasses containing 2 to 5 mol% of Nb_2O_5 and Bi_2O_3 with 12 wt% of iodine were successfully prepared without any iodine volatilization. The incorporation limit of these two crosslinking reagents into the glass network was determined. It was shown that Nb_2O_5 have a higher incorporation limit in $\text{Ag}_5\text{P}_3\text{O}_{10}$ -based glasses, while Bi_2O_3 have a higher one in AgPO_3 -based glasses, which was interpreted using the bond valence units theory. It was also shown that both Nb_2O_5 and Bi_2O_3 have higher incorporation limits in iodine-containing silver phosphate glasses than Al_2O_3 , which is consistent with the hypothesis that cations with a higher polarizability can be incorporated in higher quantity in those glasses. The increase of crosslinking reagent amount induced an increase of the glass transition temperature and of the polymerization degree of the glasses. However, the addition of iodine to these glasses led to an increase of bond lengths and bond angles, which induced a weakening of the glass network and thus a decrease of the glass transition temperature that compensates the crosslinking effect. Nonetheless, this had no effect on the polymerization degree of the glasses, which was still improved by the addition of crosslinking reagents. Moreover, no crystalline cluster of silver iodide was formed for the studied concentrations. Further work is under progress to determine if the addition of these crosslinking reagents has the expected effect on the chemical durability properties of these glasses.

6. Acknowledgments

A.-L. Chabauty thanks the CEA for PhD grant. Chevreul Institute (FR 2638), Ministère de l'Enseignement Supérieur et de la Recherche, Région Nord – Pas de Calais and FEDER are acknowledged for supporting and funding partially this work. The authors are grateful to G. Landrot from SOLEIL SAMBA beamline for his assistance with the synchrotron experiments.

7. References

- [1] Agence Nationale pour la gestion des Déchets RAdioactifs (ANDRA), Dossier Argile 2005: Tome – Safety Evaluation of a Geological Repository, Reports Series No. 270VA, ANDRA, Paris, **2005**.
- [2] M. J. Plodinec, Borosilicate Glasses for Nuclear Waste Immobilization, *Glass Technol.*, **2000**, *41*, 186-192.
- [3] F. Audubert, J. Carpena, J. L. Lacout and F. Tetard, Elaboration of an Iodine-Bearing Apatite Iodine Diffusion into a $Pb_3(VO_4)_2$ Matrix, *Solid State Ionics*, **1997**, *95*, 113-119.
- [4] A. Coulon, A. Grandjean, D. Laurencin, P. Jollivet, S. Rossignol and L. Campayo, Durability Testing of an Iodate-Substituted Hydroxyapatite Designed for the Conditioning of ^{129}I , *J. Nucl. Mater.*, **2017**, *484*, 324-331.
- [5] D.M. Strachan, H. Babad, Method for Immobilizing Radioactive Iodine, US patent No. US4229317A, **1978**.

- [6] W.E. Clark, C. T. Thompson, Immobilization of Iodine in Concrete, US Patent No. US4017417, **1977**.
- [7] T. Minami, Y. Takuma, M. Tanaka, Superionic Conducting Glasses: Glass Formation and Conductivity in the AgI-Ag₂O-P₂O₅ System, *J. Electrochem. Soc.*, **1977**, *124*, 1659-1662.
- [8] T. J. Garino, T. M. Nenoff, J. L. Krumhansl and D. X. Rademacher, Low-Temperature Sintering of Bi-Si-Zn-Oxide Glasses for use in either Glass Composite Materials or Core/Shell 129I Waste Forms, *J. Am. Ceram. Soc.*, **2011**, *94*, 2412-2419.
- [9] K. K. Olsen, J. W. Zwanziger, Multi-Nuclear and Multi-Dimensional Nuclear Magnetic Resonance Investigation of Silver Iodide-Silver Phosphate Fast Ion Conducting Glasses, *Solid State Nucl. Mag.*, **1995**, *5*, 123-132.
- [10] M. R. Reidmeyer, D. E. Day, Phosphorus Oxynitride Glasses, *J. Non-Cryst. Solids*, **1995**, *181*, 201-214.
- [11] D. E. Day, Z. Wu, C. S. Ray and P. Hrma, Chemical Durable Iron Phosphate Glass Wasteforms, *J. Non-Cryst. Solids*, **1998**, *241*, 1-12.
- [12] R. K. Brow, Nature of Alumina in Phosphate Glass: I, Properties of Sodium Aluminophosphate Glass, *J. Am. Ceram. Soc.*, **1993**, *76*, 913-918.
- [13] J. Jirak, L. Koudelka, J. Pospisil, P. Mosner, L. Montagne and L. Delevoye, Study of Structure and Properties of ZnO-Bi₂O₃-P₂O₅ Glasses, *J. Mater. Sci.*, **2007**, *42*, 8592-8598.
- [14] L. Koudelka, J. Pospisil, P. Mosner, L. Montagne and L. Delevoye, Structure and Properties of Potassium Niobato-Borophosphate Glasses, *J. Non-Cryst. Solids*, **2008**, *354*, 129-133.

- [15] C. Kim, D. E. Day, Immobilization of Hanford LAW in Iron Phosphate Glass Wasteforms, *J. Non-Cryst. Solids*, **2003**, *331*, 20-31.
- [16] T. Lemesle, F. O. Méar, L. Campayo, O. Pinet, B. Revel and L. Montagne, Immobilization of Radioactive Iodine in Silver Aluminophosphate Glasses, *J. Hazard. Mater.*, **2014**, *264*, 117-126.
- [17] T. Lemesle, Etude de matrices vitreuses aluminophosphates pour le conditionnement de l'iode radioactif, Université de Lille 1, PhD Thesis, **2013**.
- [18] T. Lemesle, L. Montagne, F. O. Méar, B. Revel, L. Campayo and O. Pinet, Bismuth-Silver Phosphate Glasses as Alternative Matrices for the Conditioning of Radioactive Iodine, *Phys. Chem. Glasses – Eur. J. Glass Sci. Tech.*, **2015**, *52*, 71-75.
- [19] N.W. Grimes, R.W. Grimes, Dielectric Polarizability of Ions and the Corresponding Effective Number of Electrons, *J. Phys. Condens. Matter*, **1998**, *10*, 3029-3034.
- [20] B. Ravel and M. Newville, ATHENA, ARTEMIS, HEPHAESTUS: Data Analysis for X-Ray Absorption Spectroscopy using IFEFFIT, *J. Synchrotron Radiat.* **2005**, *12*, 537-541.
- [21] R. M. Wenslow and K. T. Mueller, Structural Details of Aqueous Attack on a Phosphate Glass by $^1\text{H}/^{31}\text{P}$ Cross-Polarization NMR, *J. Phys. Chem. B*, **1998**, *102*, 9033-9038.
- [22] A. A. Vasileva, I.A. Nazarov, P.K. Olshin, A.V. Povolotkiy, I. A. Sokolov and A. A. Manshina, Structural Features of Silver-Doped Phosphate Glasses in Zone of Femtosecond Laser-Induced Modification, *J. Solid State Chem.*, **2015**, *230*, 56-60.

- [23] S.M. Hsu, J. J. Wu, S. W. Yung, T. S. Chin, T. Zhang, Y. M. Lee, C. M. Chu and J. Y. Ding, Evaluation of Chemical Durability, Thermal Properties and Structure Characteristics of Nb-Sr-Phosphate Glasses by Raman and NMR spectroscopy, *J. Non-Cryst. Solids*, **2012**, *358*, 14-19.
- [24] L. Koudelka, P. Kalenda, P. Mosner, L. Montagne and b. Revel, Structure-Property Relationships in Barium Borophosphate Glasses Modified with Niobium Oxide, *J. Non-Cryst. Solids*, **2016**, *437*, 64-71.
- [25] S. Daviero, L. Montagne, G. Palavit, G. Mairesse, S. Belin and V. Briois, EXAFS, XANES and ^{31}P Double-Quantum MAS-NMR of $(50-x/2)\text{Na}_2\text{O}-x\text{Bi}_2\text{O}_3-(50-x/2)\text{P}_2\text{O}_5$ Glasses, *J. Phys. Chem. Solids*, **2003**, *64*, 253-260.
- [26] R. K. Brow, R. J. Kirkpatrick, G. L. Turner, Nature of Alumina in Phosphate Glass: II, Structure of Sodium Aluminophosphate Glass, *J. Am. Ceram. Soc.*, **1993**, *76*, 919-928.
- [27] X. Zhu, C. Mai and M. Li, Effects of B_2O_3 Content Variation on the Bi Ions in Bi_2O_3 - B_2O_3 - SiO_2 Glass Structure, *J. Non-Cryst. Solids*, **2014**, *388*, 55-61.
- [28] S. H. Im, Y. H. Na, N. J. Kim, D. H. Kim, C. W. Hwang and B. K. Ryu, Structure and Properties of Zinc Bismuth Phosphate Glasses, *Thin Solid Films*, **2018**, *518*, e46-e49.
- [29] Flambard, L. Montagne, L. Delevoye, G. Palavit, J.-P. Amoureux and J.-J. Videau, Solid-state NMR Study of Mixed Network Sodium-Niobium Phosphate Glasses, *J. Non-Cryst. Solids*, **2004**, *345&346*, 75-79.
- [30] D.L. Sidebottom, Influence of Cation Constriction on the ac Conductivity Dispersion in Metaphosphate Glasses, *Phys. Rev. B: Condens. Matter Mater. Phys.*, **2000**, *61*, 14508-14516.

Table of Contents Image

